coatings

MDPI

Article

Engineering Stable and Affordable Meta-Aluminate Intercalated Mafic Hydrotalcite for Superior Bromate Remediation

Jianyu Wu * and Dongsu Bi

School of Chemical and Environmental Engineering, Shanghai Institute of Technology, Shanghai 201418, China; bidongsu@126.com

* Correspondence: wujianyu420@163.com

Abstract: In this study, one type of layered double hydroxide (LDH), the meta-aluminate intercalated mafic-modified hydrotalcite (LDH-2), was engineered through an unprecedentedly facile, affordable one-step procedure. In the interest of meticulous perception regarding our superior strategy, the conventional two-step synthesis method—the fabrication of optimal mafic-modified hydrotalcite through the coprecipitation and roasting process followed by a second aging step (LDH-1)—was also synthesized. After scrutinization of as-derived nanostructures, the adsorption capacity of both structures for bromate remediation was elaborated. When the effect of experimental variation was optimized and the impact of various ions was investigated, the more astounding performance of LDH-2 (0.97 mg/g) was detected when compared with conventional LDH-1 (0.90 mg/g). Therefore, the novel approach for the engineering of meta-aluminate intercalated mafic hydrotalcite not only introduces facile and practical procedures, but also furnishes a much more efficient adsorption system. In the matter of structure durability, the as-synthesized LDH-2 presented exceptional resistance, maintaining activity after five consecutive cycling runs. This investigation sheds light on the facile and affordable synthesis of the LDH construction.

Keywords: layered double hydroxide (LDH); bromate; adsorption; meta-aluminate; hydrotalcite

check for updates

Citation: Wu, J.; Bi, D. Engineering Stable and Affordable Meta-Aluminate Intercalated Mafic Hydrotalcite for Superior Bromate Remediation. *Coatings* **2023**, *13*, 1265. https://doi.org/10.3390/coatings13071265

Academic Editor: Maciej Fronczak

Received: 1 June 2023
Revised: 8 July 2023
Accepted: 13 July 2023
Published: 19 July 2023

Copyright: © 2023 by the authors. Licensee MDPI, Basel, Switzerland. This article is an open access article distributed under the terms and conditions of the Creative Commons Attribution (CC BY) license (https://creativecommons.org/licenses/by/4.0/).

1. Introduction

Nowadays, water remediation is considered a matter of importance, owing to the emergence of various pollutants such as pathogenic bacteria [1], excessive ions [2,3], pharmaceutical components [4,5], and so on, into water sources. During the last decades, various methods have been introduced for purifying water from such dangerous materials, including filtration processes [6,7], advanced oxidation processes [8,9], and adsorption methods [10]. When ozone technology is used to treat drinking water containing bromide ions (Br^-), a new type of contaminant, BrO_3^--based ozonation by-products, collectively known as bromate, is produced, which is classified as a class 2B potential carcinogen by the International Agency for Research on Cancer [11–13]. Currently, the most commonly used techniques for removing bromate mainly include using nanostructures under systems such as ion exchange, activated carbon adsorption, photocatalytic reduction, and so on, all of which have certain limitations in the water column [14–16].

During the last decade, enormous composites and hybrid nanomaterials have been synthesized and utilized for bromate remediation [17–19]. Layered double hydroxide (LDH) was considered one of the distinguished categories of materials, extensively utilized in diverse applications such as electrochemical demine for supercapacitors, water splitting, batteries, environmental remediation for adsorptions, and photoactive composite [20–22]. Hydrotalcites, one of the LDH family, have promising applications in the treatment of anionic pollutants in water for their unique structure and the "memory effect" of the roasted product [23–25]. Danlian Huang et al. [26] found that after synthesizing the hybrid material of ethylenediaminetetraacetic acid intercalated magnesium-aluminum type

hydrotalcite, interlayer anion exchange and surface adsorption dominated the adsorption of Cr(VI) in wastewater. Additionally, Chitrakar et al. [27,28] used Fe^{2+} and Al^{3+} in a synthesized hydrotalcite composite for the adsorption of bromate. However, it was found that bromate was reduced by Fe^{2+}, leading to the structural collapse of LDHs. To avoid this undesirable phenomenon, Huashun Ji et al. [29] used Fe^{3+} and Mg^{2+} to synthesize stabilized magnesium-iron hydrotalcite composite, otherwise known as mafic-hydrotalcite, even though the relevant adsorption properties were so weak because bromate did not intercalate into the structure. Meta-aluminate is a sightly weak acid anion and can produce sodium meta-aluminate in water through ion exchange during adsorption, making it a potential candidate for achieving exceptional performance for water purification [29,30]. The conventional synthesized process for mafic hydrotalcite is the two-step process that includes the construction of Mg–Fe Layered double oxide, followed by aging into meta-aluminate. With this in mind, in this study, an unprecedentedly facile and affordable one-step procedure was proposed.

Herein, two superior strategies were used, including the intercalation of meta-aluminate into optimized mafic-modified hydrotalcite (LDH-2) and the introduction of an unprecedently facile one-step synthesized route. The conventional synthesized process, including the construction of Mg-Fe Layered double oxide ((Mg-Fe)-LDO), followed by gaining into meta-aluminate (LHD-1), was also conducted for attaining cognition regarding our novel strategy. Consequently, both fabricated nanostructures were meticulously scrutinized, and their corresponding potential was evaluated for the treatment of bromate in drinking water. After the optimization of experimental variation and the effect of various ions on the reaction efficiency, a suitable kinetic model was proposed in detail.

2. Experimental

2.1. Reagents

Entire chemicals and solvents were purchased from Shanghai Titan Technology Co., Shanghai, China, without any modifications. Distilled water (DI water) was used throughout this study.

2.2. The Preparation of LDH-1

To achieve a mass ratio of 3 for Mg to Fe, a certain weight of $Fe(NO_3)_3 \cdot 9H_2O$ and $MgCl_2 \cdot 6H_2O$ was added into 100 mL of alkali solution, including 12.72 g of Na_2CO_3 and 4.8 g of NaOH, while vigorously stirring and maintaining the temperature condition at 30 °C. When the mixture's pH was fixed at 8.5, the temperature of solution rose to 80 °C and was continuously stirred for 2 h. Then, the temperature of the solution declined to 60 °C and was kept under immobile conditions for 20 h for gaining and crystalline. After washing and drying the acquired precipitation, the powder was roasted at 500 °C for 5 h, and the resultant was abbreviated to (Mg-Fe)-LDO. In the second stage, the specific amount of (Mg-Fe)-LDO was placed into 200 mL of an alkaline solution containing saturated meta-aluminate ions, and the temperature was increased to 85 °C under vigorous stirring for 2 h. Then, after aging for 20 h at 60 °C, the obtained precipitation was filtrated, washed, dried, and noted as LDH-2.

2.3. The Preparation of LDH-2

A total of 10 g of $NaAlO_2$, as well as the specific ratio (3) of $Fe(NO_3)_3$-$9H_2O$ and $MgCl_2 \cdot 6H2O$, was added into 200 mL of alkaline solution containing 8.2 g of NaOH. The mixture was continuously stirred for 2 h and kept at a temperature of 85 °C. Then, the solution was kept under immobile conditions for 20 h at 60 °C for aging and crystallization. At the end of the process, the precipitation was washed with DI water, dried at 120 °C for 2 h to obtain the sample, and noted as LDH-2.

2.4. Experimental Method

2.4.1. Adsorption Experiments

The absorbance was evaluated under a batch reactor with a liquid volume of 100 mL. The 1 g of specified as-synthesized nanostructure was added into the solution reaction containing 100 mL of bromate solution (1 mg/L). After a certain reaction time, 5 mL of the mixture was withdrawn, and the solid phase was separated through centrifugation for absorbance measurement. The concentrations of residual bromate were determined by an ion chromatograph (ICS-100, Dionex, USA).

2.4.2. Reusability Studies

After adsorption, the LDH-1 and LDH-2 materials were recovered by filtering the solution and washing the collected precipitate 2~3 times with DI water, followed by drying. At the next stage, 53 g of anhydrous sodium carbonate was added into a 500 mL volumetric flask; the volume was fixed with DI water and shaken well to obtain the sodium carbonate solution at a concentration of 1 mol/L. The dried LDH-1 and LDH-2 materials were added to 100 mL of sodium carbonate solution and stirred for 2 h. After 2 h, the solution was filtered, and the precipitate was washed and dried. The regenerated LDH-1 and LDH-2 were used again for five successive cycles of adsorption experiments.

3. Results and Discussion

3.1. Characterization

3.1.1. FE-SEM

As shown in Figure 1a, the LDH-1 was configurated in a lamellar structure with a regular hexagonal shape throughout the structure. However, agglomeration was obviously perceived, leading to the attachment of lamellar to pack density structure. The dense bulk of the LHD-1 made the introduction of effective surface area and mesoporosity features for successful adsorption reaction difficult. As apparent in Figure 1b, the morphological observation of LHD-2 revealed that introducing a novel synthesizing procedure did not reform the hexagonal lamellar configuration, but paves the way for rendering well-dispersion and uniform structure. Therefore, the utilization of a facile one-step fabrication process prohibits agglomeration and presents a well-uniform structure, which was considered one of the crucial steps for engineering efficient adsorbent. Moreover, a decline in the dimension of the hexagonal was conspicuously observed, through which a higher surface area was achieved.

3.1.2. XPS

XPS can directly reflect some information about the elemental composition and valence changes on the surface of the materials. The recorded survey XPS spectra of LHD-1 and LDH-2 is illustrated in Figure 1c,d, respectively. The contribution of all constitutional metal elements, including Mg, Fe, and Al, was vividly conceived, affirming the successful intercalation of meta-aluminate into mafic-hydrotalcite in the case of both LHD-1 and LDH-2.

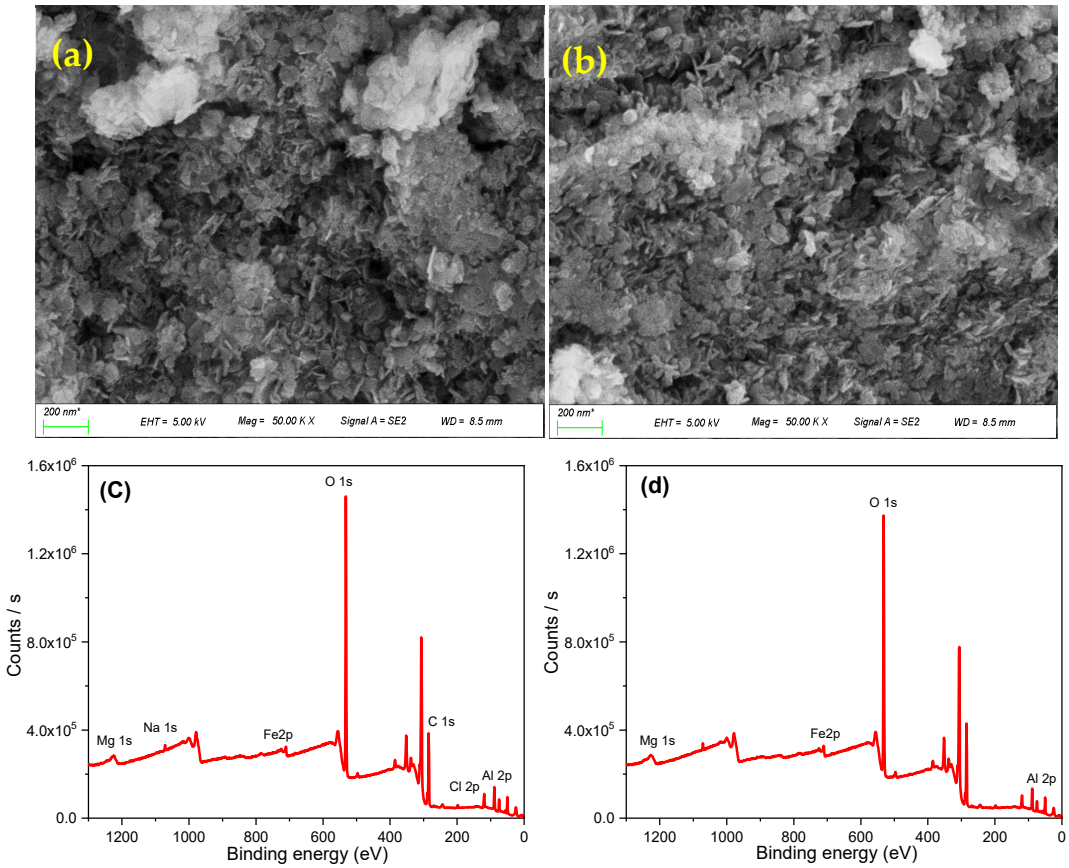


Figure 1. The FE-SEM photographs of (**a**) LHD-1, (**b**) LHD-2, the survey XPS scans of (**c**) LDH-1, and (**d**) LHD-2.

3.1.3. XRD and BET

The XRD spectra of LDH-1 and LDH-2 are shown in Figure 2a. It can be seen that both LDH-1 and LDH-2 exhibited sharp, symmetrical diffraction peaks, indicating that the samples have good and identical crystallinity. Also, the diffraction peaks at the appearing facet, including 003, 006, and 009, suggest that both LDH-1 and LDH-2 are typical Miller–Bravais, which indices the crystallized Mg-Al LDH (NO_3) phase [29,31]. As a result, the layered structure of bimetallic hydroxides is the typical type of hydrotalcite structure.

The size distribution plots of both as-synthesized adsorbents are presented in Figure 2b. The mesoporous feature of both LHD-1 and LDH-2 was meticulously confirmed owing to the majority of the porose structure being dominated in the range of 0 to 20 nm, based on the standard categorization through which the diameters of the pores must be between 2 and 50 nm. In general, adsorbents with more mesopores can effectively adsorb contaminants in water (especially in the liquid phase), adsorb large molecules well, and adsorb vapor contaminants under sufficiently high-pressure conditions using the principle of capillary coalescence [32,33]. Hence, both LDH materials have excellent adsorption properties.

The specific surface of LDH-2 was calculated to be 141.15 m^2/g, with a total pore volume of 0.2824 cm^3/g and an average pore diameter of 7.45 nm. On the other hand, the specific surface of LDH-1 was estimated to be 79.11 m^2/g, with a pore volume of 0.1577 cm^3/g and a pore diameter of 7.97 nm. In comparison, the specific surface area and total pore volume of LDH-2 are much higher than those of LDH-1. However, the pore size is slightly smaller than that of LDH-1, indicating that LDH-2 has a greater number of pore structures, and these pore structures can pave the way for LDH-2, which has a larger adsorption capacity. It is now generally accepted that the larger specific surface area and

mesoporous structure of the adsorbent tend to give higher adsorption capacity [34]. As a result, the LDHs-2 can provide more active sites for the adsorption of bromate.

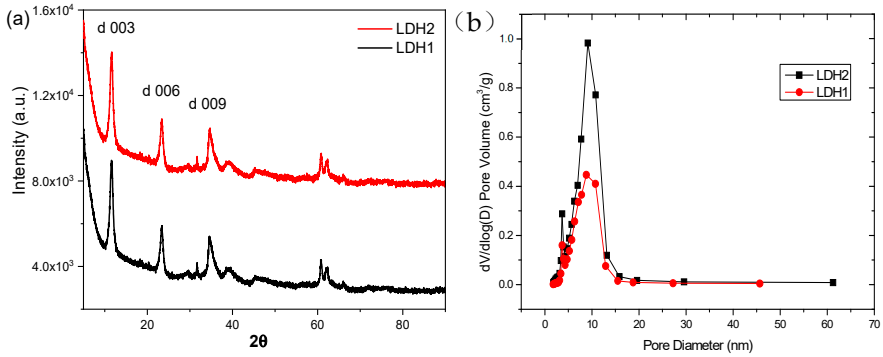


Figure 2. (**a**) XRD and (**b**) BET characterization of LDH-1 and LDH-2.

3.2. Adsorption Process

The impact of temperature on the adsorption reaction was considered of crucial importance. With this in mind, in the interest of elaborating the effect of temperature reaction on efficiency, the activity of both LDH-1 and LDH-2 was apprised under defined reaction conditions (nanostructure dosage: 1 g/L, bromate concentration: 1 mg/L, reaction time: 2 h) with an altering temperature from 30 to 80 °C. As illustrated in Figure 3a, the adsorption capacity of LDH-1 on bromate remediation increased from 0.3473 mg/g at 30 °C to 0.5795 mg/g at 80 °C. On the other hand, the adsorption capacity of LDH-2 increased from 0.3869 mg/g at 30 °C to 0.6173 mg/g at 80 °C. This output conspicuously demonstrated that the temperature dependency of the adsorption reaction on both the adsorption capacity of LDH-1 and LDH-2 has direct relation [35].

The pH-dependency of the adsorption reaction was considered another influential parameter through which the adsorption potential would be unveiled. In this regard, the reaction capability of both LDH-1 and LDH-2 was assessed by altering the primeval pH from 3 to 13. According to Figure 3b, the equilibrium adsorption capacity of LDH-1 increased from 0.250 to 0.374 mg/g by raising the pH-value from 3 to 6—the maximum equilibrium adsorption capacity. With excess increasing the pH value further than 6, the adsorption capacity was continuously quenched and reached 0.210 mg/g at a pH value of 13. Moreover, the equilibrium adsorption capacity of LDH-2 rapidly increased from 0.315 mg/g at a pH value of 3 to a pH of 5, and remained sightly unchanged between 5 and 6, at which time the equilibrium adsorption capacity was 0.4006 mg/g. When the pH value was surplus, the adsorption capacity was suppressed to 0.24 mg/g at a pH of 13. This situation could be attributed to the fact that AlO_2^- is an unstable anion, and after entering into the water body through the ion exchange function of hydrolysis, it combines with water molecules to produce $Al(OH)_3$ flocculent precipitation [36]. This phenomenon has a positive impact on the water body, and could further adsorb anionic pollutants. However, at a pH > 7, AlO_2^- would not hydrolyze after entering the water column, and consequently, the adsorption performance of bromate ions would be weakened [37,38]. At the same time, too many OH^- ions in the solution compete with bromate ions for adsorption at the higher pH value of the solution, resulting in a reduction of the positive charge on the surface of the adsorbent and weakening the adsorption performance [39].

In order to evaluate the adsorption capability of both LDH-1 and LDH-2, the bromate remediation was apprised under optimized operational variation (temperature: 25 °C and pH-value: 6) with 16 h of reaction. As apparent in Figure 3c, under the same conditions of bromate concentration, the adsorption performance of LDH-1 and LDH-2 showed rapid adsorption of bromate during the first nine hour of reactions and reached the equilibrium level. The equilibrium adsorption capacity at this time was 0.9115 mg/g, and the removal rate reached 91.15%. After a further time reaction of up to 16 h, no tangible adsorption was

detected. In the case of LDH-2, the adsorption capacity was tremendously improved up to 11 h, and then the adsorption reached its equilibrium state. The equilibrium adsorption capacity LDH-2 was detected as 0.9732 mg/g, and the removal rate reached 97.32%. LI Xin-long et al. reported that the conventional meta-aluminate intercalated mafic hydrotalcite required 14 h to reach the adsorption equilibrium with a removal rate of 91.7%.

A large number of anions exist in real wastewater effluent, which has a serious effect on the adsorption process. In this regard, systematic evaluation of the effect of various ions on the reaction efficacy is a matter of importance. In this experiment, the effect of NO_3^-, Cl^-, CO_3^{2-}, and SO_4^{2-} on the experiment was investigated. As can be seen from Figure 3d, when NO_3^- and Cl^- were added, there was almost no effect on the removal of bromate, whereas when CO_3^{2-} and SO_4^{2-} were added, the removal of bromate by both LDH-1 and LDH-2 was significantly reduced [40]. This suggests that divalent anions have a greater influence on the adsorption process rather than monovalent anions. In fact, high charge density anions are more readily adsorbed by large positive charges, similar to the results of other studies [41].

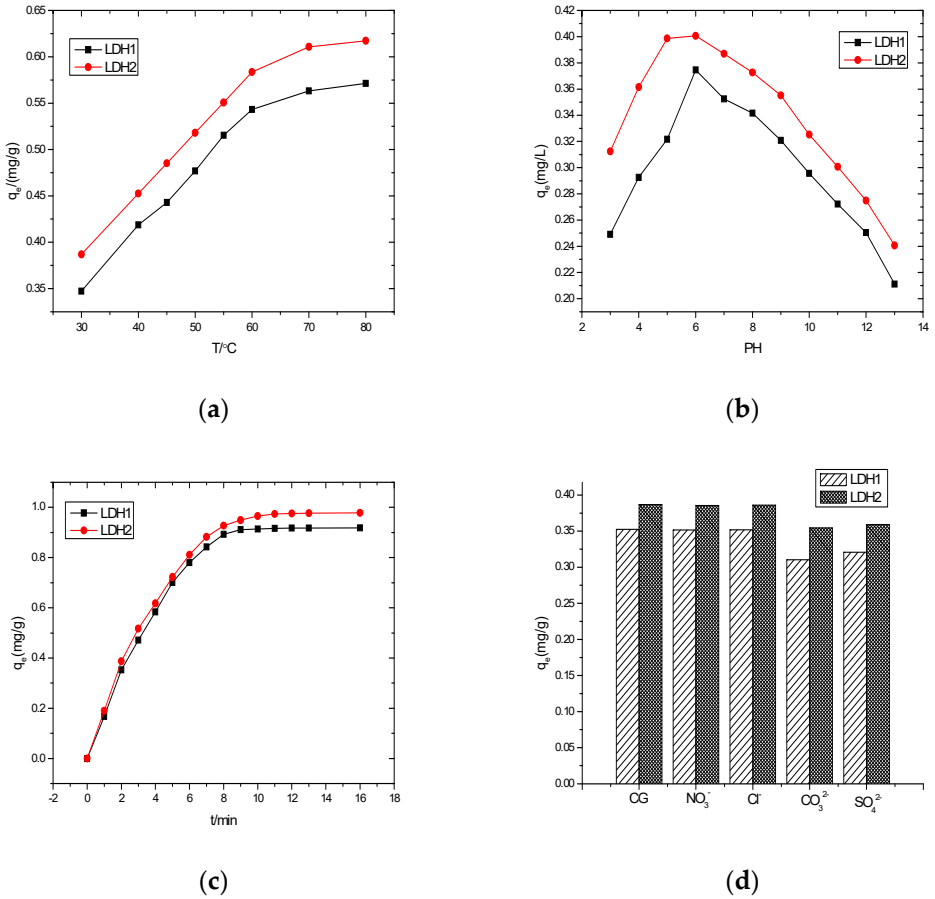


Figure 3. (**a**) The effects of temperature, (**b**) the impact of initial pH-value, (**c**) the adsorption capacity of as-synthesized samples, and (**d**) the role of coexisting various anions on reaction efficiency.

3.3. Adsorption Mechanism

The quasi-primary, quasi-secondary, Freundlich, and Langmuir kinetic models were fitted and compared to meso-LDH350; a similar material was recently reported in the literature [29], and the results are shown in Table 1. From the kinetic model data in Table 1, it can be seen that both the quasi-primary and -secondary kinetic models can perfectly describe the process of bromate adsorption under LDH-1 and LDH-2 systems. However, the fitted coefficients (R^2) attributed to the quasi-secondary kinetic model are higher than that of the quasi-primary kinetic model [42]. Therefore, the quasi-secondary

kinetic model has much more precision in describing the adsorption of bromate under both LDH-1 and LDH-2 systems, which was in line with other reported results in the literature [43]. From the viewpoint of isothermal data fitting results, it can be conceived that the maximum adsorption of LDH-1 and LDH-2 were both greater than that of the meso-LDH350 prepared by Huashun Ji et al., indicating that both LDH-1 and LDH-2 were more favorable for the adsorption of bromate. Unlike the previously reported meso-LDH350, the correlation coefficients of the Freundlich model for the LDH-1 and LDH-2 materials were greater than those of the Langmuir model, which indicated that the Freundlich model better described the process of bromate adsorption. Moreover, this behavior also indicated that the whole adsorption process was the combination of physical adsorption and chemisorption. Therefore, the Freundlich model better explained the adsorption of bromate under both LDH-1 and LDH-2 systems (rather than Langmuir) [44,45].

The adsorption mechanism can be attributed to the "memory effect" of hydrotalcite, where bromate can be adsorbed on the surface of LDH materials by physical and chemical adsorption. Since different anions have different affinities for hydrotalcite, it was shown that the affinity BrO_3^- > AlO_2^-, bringing forth that the interlayer AlO_2^- ions in LDH would be replaced by BrO_3^-, which form $NaAlO_2$ in water. Pleasingly, under acidic or neutral conditions, $Al(OH)_3$ colloidal particles precipitate and pave the way for further bromate adsorption ions in water [18].

Table 1. The adsorption kinetic models of LDH-1, LDH-2, and meso-LDH350, along with correlation coefficients of the isothermal adsorption equation.

Sorbent	Quasi-Primary Kinetic Equations			Quasi-Secondary Kinetic Equations			Freundlich Model			Langmuir Model		
	k_1	$q_{e,cal}$	R^2	k_2	$q_{e,cal}$	R^2	K_f	n	R^2	K_L	q_{max}	R^2
298K/LDH-1	0.4778	0.9376	0.9164	0.2633	0.9176	0.9838	2.86	2.50	0.9981	0.99	0.947	0.956
308K/LDH-1	-	-	-	-	-	-	2.16	2.51	0.9994	1.05	0.961	0.8837
318K/LDH-1	-	-	-	-	-	-	1.93	2.52	0.9996	1.08	0.972	0.8731
298K/LDH-2	0.4819	0.9882	0.9433	0.2834	0.9732	0.9853	2.16	2.52	0.9997	0.98	1.056	0.876
308K/LDH-2	-	-	-	-	-	-	2.07	2.54	0.9996	1.00	1.084	0.8853
318K/LDH-2	-	-	-	-	-	-	1.88	2.57	0.9998	1.05	1.108	0.8606
meso-LDH350	0.083	7.91	0.943	0.017	8.29	0.981	4.21	1.85	0.956	0.038	0.550	0.995

3.4. Reusability

Two different types of hydrotalcite materials, LDH-1 and LDH-2, were selected to study their reusability function, as presented in Figure 4. In their corresponding equilibrium adsorption capacities, the LDH-1 and LDH-2 materials maintained their initial capabilities for bromate remediation, while only a minimal decrease in the equilibrium adsorption capacities of LDH-1 and LDH-2 after five consecutive cycling runs was observed. In detail, the ignorable quenching in the performance was the reduction of 7.44 and 6.42% after five successive runs, thereby reaching the efficiency of 0.89 and 0.85%. This result indicated that the regenerated LDH-1 and LDH-2 adsorbents still have good reproducibility and continuity. In the matter of the leaching experiment after each cycle, the outcome demonstrated insignificant leached metals were observed lower than 2%, suggesting the stability of as-synthesized composites. As shown by the previous coexistence of anions, the strength of the adsorption of different anions by synthesized samples was different. In the case of sodium carbonate solutions, the bromate in the interlayer was originally replaced by carbonate in an ion exchange process [46]. This excellent reproducibility and stability means that both adsorbents may be used in large and long-term wastewater treatment applications, providing new solutions for water treatment.

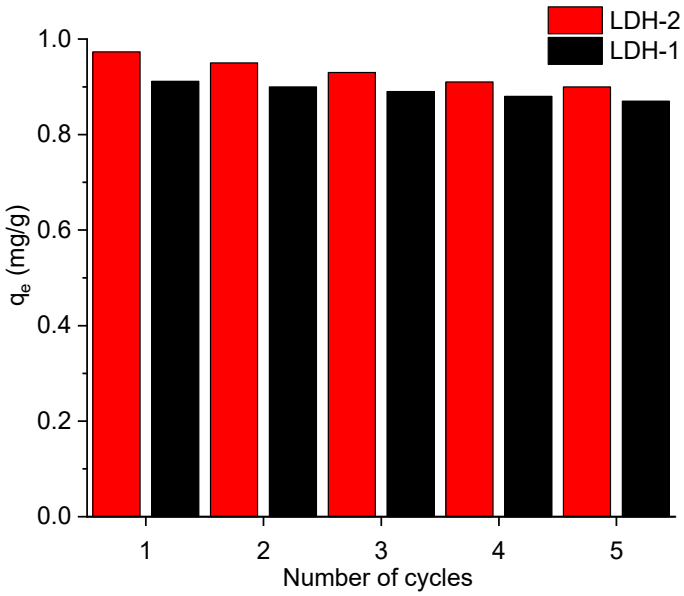


Figure 4. The reusability capability of both LDH-1 and LDH-2 samples.

4. Conclusions

In this investigation, unprecedently, the meta-aluminate intercalated mafic-modified hydrotalcite (LDH-2) was successfully fabricated through a facile and affordable synthesis route and applied for bromate remediation in water. In order to attain meticulous cognition regarding the superior structure of LDH-2, the traditional meta-aluminate intercalated mafic-modified hydrotalcite (LDH-1) was synthesized by a two-step procedure—the construction of mafic-modified hydrotalcite and the intercalation of metal-aluminate into the already formed structure. The scrutinization revealed that both LDH-1 and LDH-2 were well crystallized and formed a unitary hydrotalcite phase. However, in comparison to LDH-1, the engineering LDH-2 introduced a much more uniform lamellar configuration with a relatively smaller hexagonal shape. The textural elaboration affirmed that, in comparison with LDH-1, the LDH-2 rendered 1.8 times greater specific surface area, tremendously higher total pore volume, and a greater number of pores, all of which is in favor of efficiency enhancement. As predicted, the adsorption capacity of LDH-2 was evaluated to be 97.3% for bromate remediation in the water, while the conventional method (LDH-1) exhibited an efficiency of 91.1%. After investigating the impact of operation variations such as temperature, pH, and various ions into the reaction media, suitable kinetic models were proposed, among which both LDH-1 and LDH-2 were properly fitted with the quasi-secondary and Freundlich kinetic models. The adsorption mechanism is mainly the ion exchange between the LDH layers and the generation of $Al(OH)_3$ colloids under neutral or weakly acidic conditions, which further adsorbs bromate ions without causing secondary pollution to the water environment. The durability of as-synthesized samples was confirmed by maintaining efficient reactions through five consecutive cycling runs.

Author Contributions: J.W. and D.B.: Conceptualization, methodology, validation, formal analysis, investigation, writing—original draft preparation, writing—review and editing, visualization, and supervision. All authors have read and agreed to the published version of the manuscript.

Funding: Fund projects: Shanghai Science and Technology Innovation Action Plan Project (18DZ1203807) Subsidizing.

Institutional Review Board Statement: Not applicable.

Informed Consent Statement: Not applicable.

Data Availability Statement: All data generated or analyzed during this study are included in this published article.

Acknowledgments: Research reported in this publication was supported by fund projects: Shanghai Science and Technology Innovation Action Plan Project (18DZ1203807) Subsidizing.

Conflicts of Interest: The authors declare that they have no known competing financial interests or personal relationships that could have appeared to influence the work reported in this paper.

References

1. Wei, S.; Chen, T.; Hou, H.; Xu, Y. Recent advances in electrochemical sterilization. *J. Electroanal. Chem.* **2023**, *937*, 117419. [CrossRef]
2. Wang, Z.; Chen, C.; Liu, H.; Hrynshpan, D.; Savitskaya, T.; Chen, J.; Chen, J. Enhanced denitrification performance of *Alcaligenes* sp. TB by Pd stimulating to produce membrane adaptation mechanism coupled with nanoscale zero-valent iron. *Sci. Total Environ.* **2020**, *708*, 135063. [CrossRef] [PubMed]
3. Wang, Z.; Dai, L.; Yao, J.; Guo, T.; Hrynsphan, D.; Tatsiana, S.; Chen, J. Enhanced adsorption and reduction performance of nitrate by Fe–Pd–Fe_3O_4 embedded multi-walled carbon nanotubes. *Chemosphere* **2021**, *281*, 130718. [CrossRef]
4. Hasanvandian, F.; Shokri, A.; Moradi, M.; Kakavandi, B.; Setayesh, S.R. Encapsulation of spinel $CuCo_2O_4$ hollow sphere in V_2O_5-decorated graphitic carbon nitride as high-efficiency double Z-type nanocomposite for levofloxacin photodegradation. *J. Hazard. Mater.* **2022**, *423*, 127090. [CrossRef] [PubMed]
5. Moradi, M.; Hasanvandian, F.; Isari, A.A.; Hayati, F.; Kakavandi, B.; Setayesh, S.R. CuO and ZnO co-anchored on g-C_3N_4 nanosheets as an affordable double Z-scheme nanocomposite for photocatalytic decontamination of amoxicillin. *Appl. Catal. B Environ.* **2021**, *285*, 119838. [CrossRef]
6. Dong, S.; Zhang, H.; Yuan, D. Supramolecular Nonwoven Materials via Thermally Induced Precursor Crystallization of Nanocrystalline Fibers/Belts for Recyclable Air Filters. *ACS Appl. Nano Mater.* **2023**, *6*, 9548–9557. [CrossRef]
7. Zhao, G.; Shi, L.; Yang, G.; Zhuang, X.; Cheng, B. 3D fibrous aerogels from 1D polymer nanofibers for energy and environmental applications. *J. Mater. Chem. A* **2023**, *11*, 512–547. [CrossRef]
8. Tian, N.; Giannakis, S.; Akbarzadeh, L.; Hasanvandian, F.; Dehghanifard, E.; Kakavandi, B. Improved catalytic performance of ZnO via coupling with $CoFe_2O_4$ and carbon nanotubes: A new, photocatalysis-mediated peroxymonosulfate activation system, applied towards Cefixime degradation. *J. Environ. Manag.* **2023**, *329*, 117022. [CrossRef]
9. Heeb, M.B.; Criquet, J.; Zimmermann-Steffens, S.G.; Von Gunten, U. Oxidative treatment of bromide-containing waters: Formation of bromine and its reactions with inorganic and organic compounds—A critical review. *Water Res.* **2014**, *48*, 15–42. [CrossRef] [PubMed]
10. El-Sayed, M.E.A. Nanoadsorbents for water and wastewater remediation. *Sci. Total Environ.* **2020**, *739*, 139903. [CrossRef]
11. Fang, J.-Y.; Shang, C. Bromate formation from bromide oxidation by the UV/persulfate process. *Environ. Sci. Technol.* **2012**, *46*, 8976–8983. [CrossRef] [PubMed]
12. Ersan, M.S.; Liu, C.; Amy, G.; Karanfil, T. The interplay between natural organic matter and bromide on bromine substitution. *Sci. Total Environ.* **2019**, *646*, 1172–1181. [CrossRef] [PubMed]
13. Khan, M.R.; Wabaidur, S.M.; Alothman, Z.A.; Busquets, R.; Naushad, M. Method for the fast determination of bromate, nitrate and nitrite by ultra performance liquid chromatography–mass spectrometry and their monitoring in Saudi Arabian drinking water with chemometric data treatment. *Talanta* **2016**, *152*, 513–520. [CrossRef] [PubMed]
14. Yang, Y.; Ding, Q.; Wen, D.; Yang, M.; Wang, Y.; Liu, N.; Zhang, X. Bromate removal from aqueous solution with novel flower-like Mg-Al-layered double hydroxides. *Environ. Sci. Pollut. Res.* **2018**, *25*, 27503–27513. [CrossRef]
15. Botlaguduru, V.S.V.; Batchelor, B.; Abdel-Wahab, A. Application of UV–sulfite advanced reduction process to bromate removal. *J. Water Process Eng.* **2015**, *5*, 76–82. [CrossRef]
16. El-Hiti, G.A.; Alotaibi, M.H.; Ahmed, A.A.; Hamad, B.A.; Ahmed, D.S.; Ahmed, A.; Hashim, H.; Yousif, E. The morphology and performance of poly (vinyl chloride) containing melamine Schiff bases against ultraviolet light. *Molecules* **2019**, *24*, 803. [CrossRef] [PubMed]
17. Zhang, Z.; Hou, Z.-W.; Chen, H.; Li, P.; Wang, L. Electrochemical electrophilic bromination/spirocyclization of *N*-benzyl-acrylamides to brominated 2-azaspiro[4.5]decanes. *Green Chem.* **2023**, *25*, 3543–3548. [CrossRef]
18. Xiao, Q.; Yu, S.; Li, L.; Wang, T.; Liao, X.; Ye, Y. An overview of advanced reduction processes for bromate removal from drinking water: Reducing agents, activation methods, applications and mechanisms. *J. Hazard. Mater.* **2017**, *324*, 230–240. [CrossRef]
19. Gheonea, R.; Crasmareanu, E.C.; Plesu, N.; Sauca, S.; Simulescu, V.; Ilia, G. New hybrid materials synthesized with different dyes by sol-gel method. *Adv. Mater. Sci. Eng.* **2017**, *2017*, 4537039. [CrossRef]
20. Moradi, M.; Hasanvandian, F.; Afshar, M.G.; Larimi, A.; Khorasheh, F.; Niknam, E.; Setayesh, S.R. Incorporation of Fe in mixed CoCu-alkoxide hollow sphere for enhancing the electrochemical water oxidation performance. *Mater. Today Chem.* **2021**, *22*, 100586. [CrossRef]
21. Chaillot, D.; Bennici, S.; Brendlé, J. Layered double hydroxides and LDH-derived materials in chosen environmental applications: A review. *Environ. Sci. Pollut. Res.* **2021**, *28*, 24375–24405. [CrossRef] [PubMed]
22. Wang, Q.; O'Hare, D. Recent advances in the synthesis and application of layered double hydroxide (LDH) nanosheets. *Chem. Rev.* **2012**, *112*, 4124–4155. [CrossRef] [PubMed]

23. Hashim, N.; Sharif, S.N.M.; Hussein, M.Z.; Isa, I.M.; Kamari, A.; Mohamed, A.; Ali, N.M.; Bakar, S.A.; Mamat, M. Layered hydroxide anion exchanger and their applications related to pesticides: A brief review. *Mater. Res. Innov.* **2017**, *21*, 129–145. [CrossRef]
24. Koilraj, P.; Srinivasan, K. High sorptive removal of borate from aqueous solution using calcined ZnAl layered double hydroxides. *Ind. Eng. Chem. Res.* **2011**, *50*, 6943–6951. [CrossRef]
25. Zhu, M.-X.; Li, Y.-P.; Xie, M.; Xin, H.-Z. Sorption of an anionic dye by uncalcined and calcined layered double hydroxides: A case study. *J. Hazard. Mater.* **2005**, *120*, 163–171. [CrossRef] [PubMed]
26. Huang, D.; Liu, C.; Zhang, C.; Deng, R.; Wang, R.; Xue, W.; Luo, H.; Zeng, G.; Zhang, Q.; Guo, X. Cr (VI) removal from aqueous solution using biochar modified with Mg/Al-layered double hydroxide intercalated with ethylenediaminetetraacetic acid. *Bioresour. Technol.* **2019**, *276*, 127–132. [CrossRef]
27. Chitrakar, R.; Sonoda, A.; Makita, Y.; Hirotsu, T. Synthesis and bromate reduction of sulfate intercalated Fe (II)–Al (III) layered double hydroxides. *Sep. Purif. Technol.* **2011**, *80*, 652–657. [CrossRef]
28. Chitrakar, R.; Makita, Y.; Sonoda, A.; Hirotsu, T. Fe–Al layered double hydroxides in bromate reduction: Synthesis and reactivity. *J. Colloid Interface Sci.* **2011**, *354*, 798–803. [CrossRef]
29. Ji, H.; Wu, W.; Li, F.; Yu, X.; Fu, J.; Jia, L. Enhanced adsorption of bromate from aqueous solutions on ordered mesoporous Mg-Al layered double hydroxides (LDHs). *J. Hazard. Mater.* **2017**, *334*, 212–222. [CrossRef]
30. Barahuie, F.; Hussein, M.Z.; Abd Gani, S.; Fakurazi, S.; Zainal, Z. Synthesis of protocatechuic acid–zinc/aluminium–layered double hydroxide nanocomposite as an anticancer nanodelivery system. *J. Solid State Chem.* **2015**, *221*, 21–31. [CrossRef]
31. Valente, J.S.; Sánchez-Cantú, M.; Lima, E.; Figueras, F. Method for large-scale production of multimetallic layered double hydroxides: Formation mechanism discernment. *Chem. Mater.* **2009**, *21*, 5809–5818. [CrossRef]
32. Zhao, G.; Li, Z.; Cheng, B.; Zhuang, X.; Lin, T. Hierarchical porous metal organic framework aerogel for highly efficient CO_2 adsorption. *Sep. Purif. Technol.* **2023**, *315*, 123754. [CrossRef]
33. Hasanvandian, F.; Salmasi, M.Z.; Moradi, M.; Saei, S.F.; Kakavandi, B.; Setayesh, S.R. Enhanced spatially coupling heterojunction assembled from CuCo2S4 yolk-shell hollow sphere capsulated by Bi-modified TiO_2 for highly efficient CO_2 photoreduction. *Chem. Eng. J.* **2022**, *444*, 136493. [CrossRef]
34. Moradi, M.; Hasanvandian, F.; Bahadoran, A.; Shokri, A.; Zerangnasrabad, S.; Kakavandi, B. New high-entropy transition-metal sulfide nanoparticles for electrochemical oxygen evolution reaction. *Electrochim. Acta* **2022**, *436*, 141444. [CrossRef]
35. Chen, H.; Chen, Z.; Zhao, G.; Zhang, Z.; Xu, C.; Liu, Y.; Chen, J.; Zhuang, L.; Haya, T.; Wang, X. Enhanced adsorption of U (VI) and 241Am (III) from wastewater using Ca/Al layered double hydroxide@ carbon nanotube composites. *J. Hazard. Mater.* **2018**, *347*, 67–77. [CrossRef]
36. Wiśniewski, J.A.; Kabsch-Korbutowicz, M. Bromate removal in the ion-exchange process. *Desalination* **2010**, *261*, 197–201. [CrossRef]
37. Lv, L.; He, J.; Wei, M.; Evans, D.G.; Duan, X. Factors influencing the removal of fluoride from aqueous solution by calcined Mg–Al–CO_3 layered double hydroxides. *J. Hazard. Mater.* **2006**, *133*, 119–128. [CrossRef]
38. Dong, P.; Zhang, Y.; Zhu, S.; Nie, Z.; Ma, H.; Liu, Q.; Li, J. First-principles study on the adsorption characteristics of corrosive species on passive film TiO_2 in a NaCl solution containing H_2S and CO_2. *Metals* **2022**, *12*, 1160. [CrossRef]
39. Xiao, Q.; Wang, T.; Yu, S.; Yi, P.; Li, L. Influence of UV lamp, sulfur (IV) concentration, and pH on bromate degradation in UV/sulfite systems: Mechanisms and applications. *Water Res.* **2017**, *111*, 288–296. [CrossRef]
40. Echigo, S.; Itoh, S.; Kuwahara, M. Bromide removal by hydrotalcite-like compounds in a continuous system. *Water Sci. Technol.* **2007**, *56*, 117–122. [CrossRef]
41. Goh, K.-H.; Lim, T.-T.; Dong, Z. Application of layered double hydroxides for removal of oxyanions: A review. *Water Res.* **2008**, *42*, 1343–1368. [CrossRef] [PubMed]
42. Xu, J.; Lan, W.; Ren, C.; Zhou, X.; Wang, S.; Yuan, J. Modeling of coupled transfer of water, heat and solute in saline loess considering sodium sulfate crystallization. *Cold Reg. Sci. Technol.* **2021**, *189*, 103335. [CrossRef]
43. Bagherifam, S.; Komarneni, S.; Lakzian, A.; Fotovat, A.; Khorasani, R.; Huang, W.; Ma, J.; Wang, Y. Evaluation of Zn–Al–SO_4 layered double hydroxide for the removal of arsenite and arsenate from a simulated soil solution: Isotherms and kinetics. *Appl. Clay Sci.* **2014**, *95*, 119–125. [CrossRef]
44. Zhang, Y.; Jing, S.; Liu, H. Reactivity and mechanism of bromate reduction from aqueous solution using Zn–Fe (II)–Al layered double hydroxides. *Chem. Eng. J.* **2015**, *266*, 21–27. [CrossRef]
45. EM, A.E.-M.; Eltaweil, A.S.; El-Subruiti, G.M.; Mohy-Eldin, M.S.; Omer, A.M. Adsorption of nitrophenol onto a novel Fe_3O_4-κ-carrageenan/MIL-125 (Ti) composite: Process optimization, isotherms, kinetics, and mechanism. *Environ. Sci. Pollut. Res. Int.* **2023**, *30*, 49301–49313.
46. Wang, L.; Zhang, J.; Liu, J.; He, H.; Yang, M.; Yu, J.; Ma, Z.; Jiang, F. Removal of bromate ion using powdered activated carbon. *J. Environ. Sci.* **2010**, *22*, 1846–1853. [CrossRef]

Disclaimer/Publisher's Note: The statements, opinions and data contained in all publications are solely those of the individual author(s) and contributor(s) and not of MDPI and/or the editor(s). MDPI and/or the editor(s) disclaim responsibility for any injury to people or property resulting from any ideas, methods, instructions or products referred to in the content.